LONDON
SCHOOL *of*
HYGIENE
&TROPICAL
MEDICINE

Bacterial Virulence Factor Inhibits Caspase-4/11 Activation in Intestinal Epithelial Cells

Mitchell A. Pallett[1], **Valerie F. Crepin**[1], **Nicolas Serafini**[2,3], **Maryam Habibzay**[1], **Olga Kotik**[1], **Julia Sanchez-Garrido**[4], **James P. Di Santo**[2,3], **Avinash R. Shenoy**[4], **Cedric N. Berger**[1], and **Gad Frankel**[1,#]

[1]Department of Life Sciences, MRC Centre for Molecular Bacteriology and Infection, Imperial College London, UK

[2]Innate Immunity Unit, Institut Pasteur, Paris, France

[3]Inserm U668, Paris, France

[4]Department of Medicine, MRC Centre for Molecular Bacteriology and Infection, Imperial College London, UK

Abstract

The human pathogen enteropathogenic *Escherichia coli* (EPEC), as well as the mouse pathogen *Citrobacter rodentium*, colonize the gut mucosa via attaching and effacing lesion formation and cause diarrheal diseases. EPEC and *C. rodentium* type III secretion system (T3SS) effectors repress innate immune responses and infiltration of immune cells. Inflammatory caspases such as caspase-1 and caspase-4/11 are crucial mediators of host defense and inflammation in the gut via their ability to process cytokines such as IL-1β and IL-18. Here we report that the effector NleF binds the catalytic domain of caspase-4 and inhibits its proteolytic activity. Following infection of intestinal epithelial cells (IECs) EPEC inhibited caspase-4 and IL-18 processing in an NleF-dependent manner. Depletion of caspase-4 in IECs prevented the secretion of mature IL-18 in response to infection with EPEC *nleF*. NleF-dependent inhibition of caspase-11 in colons of mice prevented IL-18 secretion and neutrophil influx at early stages of *C. rodentium* infection. Neither wild-type *C. rodentium* nor *C. rodentium nleF* triggered neutrophil infiltration or IL-18 secretion in *Cas11* or *Casp1/11* deficient mice. Thus, IECs play a key role in modulating early innate immune responses in the gut via a caspase-4/11 - IL-18 axis, which is targeted by virulence factors encoded by enteric pathogens.

#Corresponding author, Gad Frankel, MRC CMBI, Flowers Building, Imperial College, London, SW7 2AZ, g.frankel@imperial.ac.uk.

Keywords

Caspase-4/11; Citrobacter rodentium; NleF; type III secretion system; intestinal epithelial cells

Introduction

Central to the infection strategy of the extracellular pathogens enteropathogenic *Escherichia coli* (EPEC), enterohaemorrhagic *E. coli* (EHEC)(1) and *Citrobacter rodentium*(2) is injection of type III secretion system effectors into intestinal epithelial cells (IECs) where they target diverse signalling pathways, particularly innate immune signaling. NleC and NleD are Zn-dependent endopeptidases that specifically cleave and disable RelA (p65) and JNK, respectively, thus blocking NF-κB and AP-1 activation(3). NleE is a methyltransferase that specifically modifies a cysteine in the zinc finger domain of TAB2 and TAB3 thus also blocking NF-kB signalling(4). NleB, which also inhibits NF-kB, has an N-acetylglucosamine transferase activity that specifically modifies Arg 117 in the death domain of FADD(5,6) and NleH is a serine/threonine kinase that inhibits the RPS3/NF-κB pathway via phosphorylation of CRKL (v-Crk sarcoma virus CT10 oncogene-like protein) (7).

Inhibition of innate immunity by EPEC and EHEC is needed to counter its activation by the T3SS, flagellins and lipopolysaccharides (LPS), which are readily detected by sensors and receptors in mammalian hosts. In response to infection, some sensors assemble macromolecular complexes called inflammasomes to stimulate the protease activity of caspase-1. The proteolytic processing and release of interleukin (IL)-1β and IL-18, and the induction of pyroptotic cell death triggered by caspase-1 can prevent the establishment and spread of microbial pathogens(8,9). In addition, the single mouse caspase-11 and the related human caspase-4 and caspase-5 act as cytosolic receptors, which bind LPS directly via their N-terminal caspase activation and recruitment domains (CARD, p22 domain). LPS binding induces oligomerization and autoproteolytic activation of caspase-4/5/11 into their active p20/p10 fragments and subsequent pyroptotic lysis of bacterially infected host cells(10). In human and mouse phagocytic cells LPS is detected by caspase-4/11, which stimulate caspase-1-dependent maturation of IL-1β and IL-18 via the NLRP3-ASC inflammasome(11–13). However, in IECs caspase-4/11 acts independently of NLRP3 and caspase-1 to directly process IL-18 and induce pyroptosis during *Salmonella* infection(14). Therefore the detection of Gram-negative bacteria by IECs markedly contrasts that in myeloid cells. However, unlike *Salmonella*, which are intracellular pathogens, extracellular pathogens use T3SS to prevent death pathways in host cells to which they intimately adhere(5,6,15). This suggests that EPEC, EHEC and *C. rodentium* might manipulate caspase-4/11 and/or inflammasome pathways in IECs.

Previous work on *C. rodentium* infections in mice showed that loss of inflammasome signaling related genes such as *Nlrp3, Nlrc4, Casp1, Casp11, Il1β* and *Il18* results in enhanced morbidity and inflammatory disease, whereas wild-type mice clear the pathogen within 14-21 days(16,17). Detection of *C. rodentium*, EHEC and EPEC in myeloid cells has also been studied previously, and a recent report identified the EPEC NleA T3SS effector

protein as an inhibitor of NLRP3-caspase-1 inflammasomes(18). However, as IECs use non-canonical, NLRP3- and caspase-1-independent mechanisms to detect bacteria, we hypothesized that EPEC and *C. rodentium* subvert caspase-4/11 action in IECs upon initial attachment. Here we report that bacterial T3SS effector NleF is a potent inhibitor of mammalian caspase-4/11 and thus prevents IL-18 secretion from IECs *in vitro,* and blocks caspase-11 – IL-18 mediated neutrophil influx during infection *in vivo.*

Results

NleF binds human caspase-4

The highly conserved effector NleF was previously reported to bind the active site and to inhibit the activity of caspase-9, caspase-8 and caspase-4, however, whether NleF affects inflammasome signaling and the innate immune response to bacterial infection *in vivo* has not been tested(19). By employing a yeast-2-hybrid screen (Table S1) and a direct yeast-2-hybrid (DYH) assay (Fig. 1A) we confirmed that human caspase-4 is an interacting partner of EPEC NleF (NleF$_{EPEC}$). Truncation analyses revealed an interaction between NleF$_{EPEC}$ and the p30 catalytic domain of caspase-4 (Fig. 1B). Deletion of four C-terminal residues in NleF$_{EPEC}$ (NleF$_{1-185\_EPEC}$) abrogates its binding to caspase-9(19), and similar defects were seen in binding to caspase-4 (Fig. 1B). Mutation of the substrate-binding pocket of caspase-4 (R152A, W313A and R314A) also abolished NleF-caspase-4 interaction (Fig. 1B). To confirm that the binding is direct, the caspase-4 p20 subunit (22 kDa; His tagged), p10 subunit (10 kDa) and NleF$_{EPEC}$ (65 kDa; MBP fusion) were co-expressed, purified by tandem affinity chromatography and analyzed by gel filtration. Three chromatographic peaks corresponding to free MBP-NleF$_{EPEC}$, free His-p20, and a complex containing NleF$_{EPEC}$, p20 and p10 subunits were observed (Fig. 1C). NleF$_{EPEC}$ and caspase-4 subunits co-purified and co-eluted as a macromolecular complex with an apparent molecular weight (MW) of ~230 kDa (Fig. 1C-D).

NleF inhibits human caspase-4 and mouse caspase-11

Recombinant caspase-4 underwent auto-proteolytic activation presumably as a consequence of LPS binding when purified from *E. coli.* Wild-type caspase-4, but not a catalytic dead mutant (caspase-4C285S), underwent auto-proteolysis to the active p20 form and hydrolyzed the caspase-4 fluorogenic substrate peptide (Ac-LEVD-AFC; Fig. 2A). Recombinant NleF$_{EPEC}$ inhibited the activity of caspase-4 in a dose-dependent manner with an IC$_{50}$ of 5 nM (Fig. 2B), comparable to 14 nM previously measured for NleF$_{EHEC}$ by Blasche et al. (19). Despite not binding caspase-4 in DYH, NleF$_{1-185\_EPEC}$, which was pulled down with caspase-4 at low levels (data not shown), was able to inhibit caspase-4 activity although at an IC$_{50}$ of 25.5 nM (Fig. 2B). *C. rodentium* NleF (NleF$_{CR}$), which shares 84% amino acid identity with NleF$_{EPEC}$, strongly inhibited the proteolytic activity of mouse caspase-11 (IC$_{50}$ of 13 nM; Fig. 2C-D) revealing an evolutionarily conserved functional property. Importantly, we found that NleF$_{EPEC}$ inhibits caspase-4 more efficiently than NleF$_{CR}$ (Fig. 2C), while NleF$_{CR}$ inhibits caspase-11 more efficiently than caspase-4 (Fig. 2F).

NleF inhibits h-caspase-4 activation during infection

To investigate if NleF$_{EPEC}$ targets caspase-4 during infection of human IECs, Caco-2 cells were infected with the wild-type (WT) EPEC and EPEC *nleF*; both strains adhered to the cultured cells equally (Fig. 3A). However, while secreted caspase-4 was absent following infection with WT EPEC, the active p30 fragment of caspase-4 was found in the supernatants of cells infected with EPEC *nleF* (Fig. 3B). Addition of the caspase-4 inhibitor Ac-LEVD-CHO complemented the EPEC *nleF* phenotype in a dose dependent manner (Fig. 3B).

NleF$_{EPEC}$ did not affect the expression of pro-IL-18, which was similar in uninfected cells and those infected with all the EPEC strains (Fig. 3C). While secretion of pro-IL-18 was detected upon infection with WT EPEC and EPEC *nleF*, pro-IL-18 was only processed into the active form following infection with EPEC *nleF* (Fig. 3D). Secretion of mature IL-18 (mIL-18), induced by EPEC *nleF*, was not detected when this strain was complemented with a plasmid encoding NleF$_{EPEC}$ (pNleF$_{EPEC}$) (Fig. 3D).

To confirm that inhibition of caspase-4 by NleF was sufficient to block processing of IL-18, we generated Caco-2 cells depleted of caspase-4 using miRNA30E based stable shRNA expression (Fig. 4A). EPEC *nleF* infection of Caco-2 cells silenced for caspase-4 expression (C4) did not secrete mIL-18, as measured by both western blotting (Fig. 4B) and ELISA (Fig. 4C), clearly pointing to a requirement of caspase-4 in IL-18 processing during EPEC infection of IECs. Importantly, no cell death was detectable by measuring LDH release or PI uptake following infection of control or caspase-4-depleted Caco-2 cells (Fig. 4D); this is likely due to EPEC T3SS effectors (e.g. NleH, NleB), which inhibit cell death(5,6,15). Thus, in human IECs, pro-IL-18 processing during EPEC infection is caspase-4 dependent and the bacterially injected NleF specifically inhibits this process.

C. rodentium inhibits IL-18 secretion *in vivo* in an NleF$_{CR}$-dependent manner

To test the role of NleF during infection *in vivo* we infected C57BL/6 mice with WT *C. rodentium*, *C. rodentium nleF* or *C. rodentium nleF* complemented with p*nleF*$_{CR}$. Colonization (Fig. 5A) and colonic crypt hyperplasia (Fig. 5B) were similar between the different *C. rodentium* strains (Fig. 5). We quantified levels of IL-18 and IL-1β secreted from colonic explants, and the inflammasome-independent chemokine CXCL1 as a control, on days 4 and 8 post-infection (p.i.). On day 4 post infection of C57BL/6 mice with *C. rodentium nleF* we detected a significantly increased colonic secretion of IL-18, while mock-infected (PBS) or WT *C. rodentium*-infected colons released similarly low levels of IL-18 (Fig. 5C). Complementing the *C. rodentium nleF* mutant with a plasmid encoding NleF$_{CR}$ restored the inhibition of IL-18 secretion (Fig. 5C); secreted IL-1β was below the detectable limit (data not shown). Secretion of CXCL1 was similar in colons extracted from mice treated with PBS or infected with WT *C. rodentium* or *C. rodentium nleF* (Fig. 5D). Complementing the *C. rodentium nleF* mutant with a plasmid encoding NleF$_{CR}$ resulted in a significantly increased CXCL1 secretion (Fig. 5D), which is consistent with our recent finding that over expression of NleF$_{EPEC}$ activates NF-κB in cultured cells(20). Importantly, NleF-dependent inhibitory effects were only observed early during infection (day 4 p.i.), and

IL-18 secretion was similar following WT *C. rodentium* or *C. rodentium nleF* infection on day 8 p.i. (Fig. 5E).

To validate that NleF$_{CR}$ inhibits IL-18 secretion via the inflammasomes, we first infected *Casp1/11* deficient mice with *C. rodentium* and *C. rodentium nleF*. As expected, loss of *Casp1* and *Casp11* abolished IL-18 secretion from colonic explants after infection with WT *C. rodentium* or *C. rodentium nleF* (Fig. 5C); CXCL1 secretion was similar in *Casp1/11⁻/⁻* mice infected with the two strains (data not shown). In order to confirm that the phenotype was due to caspase-11, we next infected *Casp11⁻/⁻* mice with *C. rodentium* or *C. rodentium nleF*. This showed that while WT *C. rodentium* and *C. rodentium nleF* colonized the *Casp11⁻/⁻* mice at comparable levels (Fig. 5F), secretion of IL-18 was extremely low and similar to that in *Casp1/11⁻/⁻* mice (Fig. 5C). We therefore concluded that caspase-11 is responsible for secretion of IL-18 following infection with *C. rodentium nleF*.

IL-18 is essential for the recruitment of neutrophils early during *C. rodentium* infection

As IL-18 facilitates neutrophil and leukocyte recruitment to sites of inflammation(21), we investigated the effect of NleF$_{CR}$ on immune cell recruitment. Infection of C57BL/6 mice for 4 days with *C. rodentium nleF* resulted in a significant increase in neutrophil recruitment in comparison to WT *C. rodentium*-infected or PBS-treated mice (Fig. 6B). Infection with the *C. rodentium nleF* p*nleF*$_{CR}$ strain restored the inhibition of neutrophil recruitment (Fig. 6B). No significant differences were observed for other myeloid or lymphocyte cell type analyzed, including macrophages, ILC, B-cells and T-cells (data not shown). Furthermore, correlating with similar IL-18 secretion, no difference in neutrophil recruitment was observed at day 8 post infection (Fig. 6C), suggesting that NleF$_{CR}$ plays a specific role during early immune responses to *C. rodentium*. Enhanced neutrophil influx was *Casp1/11* dependent; absence of these caspases abolished the increase in neutrophil recruitment during infection with *C. rodentium nleF* (Fig. 6B). Similar results were obtained following infection of *Casp11⁻/⁻* mice (Fig. 6B). Thus NleF$_{CR}$ is a virulence factor responsible for early inhibition of the host inflammasomes, and that the inflammasome is essential for early neutrophil recruitment in response to *C. rodentium* infection.

Discussion

Inflammasome dependent cytokines and pyroptosis have important antimicrobial functions(8,9). It is therefore not surprising that pathogenic bacteria have evolved mechanisms to prevent inflammasome activation(22). For example, *Yersinia* uses YopK to prevent detection of its T3SS(22), and bacteria modify their LPS to evade detection by caspase-11(23). The *Shigella flexneri* effector OspC3 sequesters caspase-4 activity by binding the caspase-4 p20 subunit to prevent p10 binding and oligomerization(24). Here we demonstrate that a virulence factor of A/E pathogens, NleF, targets the heterotetramer complex of caspase-4 via its C-terminal motif, underlining the importance of caspase-4 inhibition during the course of infection.

In agreement with our biochemical analyses, EPEC was able to inhibit caspase-4 in IECs in an NleF-dependent manner, while recent reports showed that infection of cultured cells with either *Salmonella* or EPEC led to caspase-4 activation(24) and caspase-4-dependent

induction of IL-18 release(14). Taken together, our data suggest that while EPEC can initiate caspase-4 activation and IL-18 processing, NleF dampens this response. Previous studies have shown that *Nlrp3, Nlrc4, Casp1* and *Casp11* are important in protection against *C. rodentium* infection(16,25). Loss of inflammasome-related genes results in significantly increased *C. rodentium* bacterial load in the intestine late in infection, which may partly explain the enhanced inflammation in inflammasome-deficient mice infected with *C. rodentium.* Loss of inflammasome-dependent IL-1β and IL-18 also results in enhanced bacterial burdens at late stages of infection and susceptibility to *C. rodentium* infection of *Il1b*^{-/-} and *Il18*^{-/-} mice(16). Our studies establish that NleF functions at early stages of infection of mucosal surfaces by inhibiting the inflammasome and preventing release of IL-18 by epithelial cells.

We also found that $NleF_{CR}$ inhibited caspase-11-dependent neutrophil recruitment. IL-18 is a key regulator of the adaptive immune response, stimulates the migration of innate and adaptive immune cells(21,26,27), and controls intestinal epithelial cell turnover and protects against damage in the intestine(28). During the early stages of infection, IL-18 is largely secreted by epithelial cells(17). Current data(16), including the secretion of IL-1β which is not expressed in non-hematopoietic cells(29), suggests that at later time points during *C. rodentium* infection colonic IL-18 secretion may switch to be myeloid cell dependent(16). Therefore, myeloid cell secretion of the IL-1 family cytokines may not be subverted by $NleF_{CR}$ and would become the pre-dominant source of IL-18 and IL-1β at the peak of infection. Similarly secretion of IL-22 is switched from ILC3 at early phase of infection to IL-22-producing T cells at later time points (> 7 days)(30).

The study demonstrates a pathway during infection of IECs, which leads to the activation of caspase-11, secretion of IL-18 and recruitment of neutrophil. In addition, we show that inhibition of caspase-11 by bacterial NleF blocks this pathway in the host. Our findings are consistent with the recent study on the epithelial cell caspase-11–IL-18 axis during *Salmonella* infection, which reported significant neutrophil influx in infected gall bladder epithelia of wild-type mice, but no neutrophil influx in *Casp11*^{-/-} mice(31).

Recent studies have revealed the contribution of non-inflammasome and inflammasome-forming NLRs in the non-hematopoietic compartment for intestinal homeostasis and the host mediated clearance and protection against enteric pathogens(35). Mice deficient in NLRP6 have impaired goblet cell mucus exocytosis and display a microbiome exposed epithelial cell layer and persistence of *C. rodentium* infection(36). Moreover, NLRP12 is a checkpoint for non-hematopoietic non-canonical NF-κB activation(37), and acts as a negative regulator of colitis and colitis-associated colon cancer. Furthermore, IEC-expressed NLRC4 mediates early innate immune responses against *C. rodentium* via an unknown mechanism independent of IL-1 family cytokine secretion(38). Here we show that the caspase-4/11 dependent IECs inflammasome is crucial for IL-18 cytokine maturation and the early innate immune response to EPEC/ *C. rodentium.* Consistently with this, Song-Zhao et al.(17) recently suggested, based on studies of *Nlrp3*^{-/-} and *Asc*^{-/-} mice, that early protection to *C. rodentium* infection is mediated by IECs independently of NLRP3 activation. Taken together, our study identifies a fundamental and novel role for the T3SS effector NleF in the

pathogenesis and virulence of A/E pathogens through the inhibition of the newly characterized IECs caspase-4/11 dependent inflammasome.

Methods

Strains, oligonucleotides, plasmids and antibodies

Strains, plasmids and primers used in this study are listed in Tables S2-S3 respectively. *nleF* was amplified from EPEC E2348/69 and *C. rodentium* ICC169 genomic DNA by PCR. Site-directed mutagenesis was carried out by inverse PCR using KOD Hot Start polymerase and mismatch primers. All constructs were confirmed by sequencing (GATC biotech). For Western Blot, Mouse monoclonal anti-caspase-4 clone 4B9 (sc-56056; Santa Cruz), anti-α-Tubulin clone DM1A (T6199), mouse polyclonal antibody anti-caspase-11 p20 clone A-2 (sc-374615; Santa cruz) and anti-pro-IL-18 (CPTC-IL18-1; DSHB), the rabbit monoclonal anti-IL-18 (PM014; MBL), anti-caspase-5 (4429; Cell signalling) and the rabbit polyclonal antibody anti-GFP (Ab290; Abcam) were used as primary antibodies. Horse radish peroxidase (HRP)-conjugated goat anti-rabbit IgG (Fc fragement; catalog no.111-035-008; Jackson immunoresearch) and HRP-conjugated goat anti-mouse IgG (Fc fragement; catalog no, 115-035-008; Jackson immunoresearch) were used as secondary antibodies.

Retroviral transductions and stable knockdown cell lines

Micro-RNA30 based (miR-30; Table S1) gene silencing constructs were generated in pMX-CMV-YFP using one-step sequence and ligation independent cloning (SLIC) (36) following the optimized miR-30E vector design(39). Sequences were as follows: *CASP4* - CGACTGTCCATGACAAGAT; and *LacZ* (non-targeting negative control) ACGTCGTATTACAACGTCGTGA. The miR-30E plasmids were transfected using Lipofectamine 2000 (Invitrogen), along with the packaging plasmids pVSV-G and pCMV-MMLV-pack(40) into HEK293E cells to produce a VSV-G pseudotyped retroviral particles for transduction. After 48 h supernatants were filtered through 0.45 μm syringe filters and added directly to pre-seeded Caco-2 TC7 cells. Transduced cells were selected by puromycin (Gibco Invitrogen) at 10 μg.ml^{-1} and knockdown was confirmed by western blotting.

EPEC infection, ELISA and Western blotting

Caco-2 TC7 cells (ATCC) were seeded at 7.5 x10^4/ml and upon reaching confluence (7 days) the medium was changed every day for 7 the following 7 days. Before infection the cells were starved for 3 h in serum free DMEM. Monolayers were infected with primed EPEC(20) at an MOI of 1:10 for 3 h. The cells were then washed twice in PBS and the medium was replaced with serum free DMEM-high glucose plus penicillin and streptomycin at 100 U/ml and 100 μg/ml, respectively. After 1 h cells were washed and either processed for Western Blot (total IL-18) or incubated for a further 17 h (secreted caspase-4 and IL-18) with or without Ac-LEVD-CHO (Enzo Lifesciences). Supernatants were collected, cleared by centrifugation at 13000 rpm at 4 °C for 10 min and precipitated for Western blotting with the addition of 10 % (v/v) trichloroacetic acid for 17 h at 4 ºC. The concentration of IL-18 in cell supernatant (MBL) was determined by ELISA according to the manufacturer's protocol.

Cell adhesion and cytotoxicity assays

Caco-2 TC7 were infected with the WT EPEC, EPEC *nleF* and the complemented strain (p*nleF*EPEC) for 3 h. The monolayers were lysed in 1 % PBS/triton X-100 and EPEC attachment was enumerated by serial dilution on LB-Agar and calculation of colony forming units (CFU).

Supernatants of uninfected cells or cell infected with EPEC for 21 h were harvested and the level of LDH release was measured using CytoTox 96® Non-Radioactive Cytotoxicity Assay (Promega). As a control for total LDH, cell lysis buffer (1 % Triton-X100/ PBS) was added for 30 min at 37 ℃ directly to the medium and cell layer. Absorbance was measured at 490 nm using the FluoStar Omega plate reader and results are displayed as percentage of total release corresponding to the LDH measured in the supernatant divided by the total LDH.

Alternatively the media was removed and cell layers were incubated in 3.3 μg/ml propidium iodide (Invitrogen) in warm PBS (PI/PBS) for 15 min and fluorescence was measured at an excitation of 510 nm and emission of 610 nm using the FluoStar Omega plate reader. As a control PI/PBS alone was measured or cell lysis buffer (0.05 % Triton X-100/PBS) supplemented with 3.3 μg/ml propidium iodide was added for 15 min at 37℃. Results are displayed as a percentage of total PI uptake.

Yeast-2-hybrid screen and yeast direct hybrids

A yeast-2-hybrid screen was conducted using pGKBT7-*nleF*$_{EPEC}$ and the HeLa cell cDNA Library following the manufacturer's Handbook (Clontech). AH109 were co-transformed with pGBT9-*bait* and pGADT7-*prey* (Table S3) and plated onto Difco Yeast Nitrogen Base without amino acids (SD) agar supplemented with 2% glucose, 20 mg/L adenine hemisulfate, 20 mg/L arginine HCl, 20 mg/L histidine HCl monohydrate, 30 mg/L isoleucine, 30 mg/L lysine HCl, 20 mg/L methionine, 50 mg/L phenylalanine, 200 mg/L threonine, 30 mg/L tyrosine, 20/L mg uracil, 150 mg/ml valine and lacking tryptophan and leucine (Double Drop-out; DDO) for selection of transformed clones. Clones positive for both plasmids were re-streaked on to SD DDO and SD QDO /-His/-Ade supplemented with 40 mg/L x-α-gal (SD QDO) for selection of positive interactions.

Recombinant Protein expression and purification

E. coli BL21 Star expressing pET28-NleF$_{EPEC}$ (pICC1659), pET28-NleF$_{1-185-EPEC}$ (pICC1660) and pET28-NleF$_{CR}$ (pICC1839) were cultured for 16 h in LB at 37 °C at 200 rpm. Bacteria were sub-cultured at 1:100 into 1 L LB supplemented with 50 μg/ml kanamycin and incubated at 37°C at 200 rpm until OD$_{600}$ of 0.4-0.6. Cultures were then induced with 0.5 mM IPTG for 18 h at 18°C. Cells were harvested by centrifugation at 10000 rpm for 20 min and re-suspended in 30 ml ice cold His-lysis buffer (20 mM Tris-HCl pH 7.9, 0.5 M NaCl, and 5 mM Imidazole). The cells were lysed by Emulsiflex following the manufacturer's instructions (Emulsiflex-B15; Avestin) and centrifuged at 14000 rpm for a further 30 mins at 4°C. Supernatant was removed and applied to 5 ml His resin (Novagen) pre-charged in 5 mM NiSO$_4$ and pre-equilibrated in His-lysis buffer and rocked at 4°C for 1.5 h. Samples were applied to a Poly-Prep Chromatography column (Qiagen) and flow-

through was collected. The column was washed twice with 20 ml His-lysis buffer and once in 20 ml wash buffer (Tris-HCl pH 7.9, 0.5 M NaCl, and 60 mM Imidazole). His-tagged fusion proteins were eluted with 10 x 1 ml elution buffer (His-lysis buffer supplemented with 1 M Imidazole). Fractions containing His-purified NleF were checked by SDS-PAGE gel electrophoresis and further purified by size exclusion (Akta prime) with a Superdex75 column (GE Healthcare; 10/300GL).

Co-purification of the caspase-4-NleF$_{EPEC}$ complex

BL21 Star cells were co-transformed with pACYC-DUET-1-$CASP4^{C258S}$ His-p20/p10 and pMAL-c2x-$nleF_{EPEC}$. Bacterial pellets were re-suspended in 20mM Tris-HCl pH 7.4, 250 mM NaCl and lysed by sonication and purified by amylose affinity chromatography. Bacterial lysates were incubated with amylose resin for 1.5 h at 4 °C and then washed with 50 ml wash buffer (20 mM Tris-HCl pH 8.0, 250 mM NaCl and eluted with wash buffer supplemented with 10 mM maltose. The co-elute was dialysed and then purified further by IMAC talon affinity chromatography, as described previously(41). Complex formation was analysed by size exclusion (Akta prime) with a Superdex200 column (GE Healthcare) using the Gel Filtration Markers Kit for Protein Molecular Weights 12,000-200,000 Da (Sigma-Aldrich) to determine complex size. Size exclusion fractions were verified by SDS PAGE gel and confirmed by Mass spectrometry.

Caspase activity assays

BL21 star were transformed with pET28a-empty, pET28a-$CASP4$, pET28a-$CASP4$ C258S or pET28a-$Casp11$. Soluble lysates at 200 μg/ml were incubated with or without 50 μM Ac-LEVD-AFC (Enzo Life Sciences) in 20 mM PIPES, 100 mM NaCl, 10 mM DTT, 1 mM EDTA, 0.1% CHAPS, 10% sucrose pH 7.2 or 20 mM Tris, 250 mM NaCl pH 7.4 for caspase-11 and caspase-4, respectively. Purified recombinant His-NleF derivatives were added at varying concentrations from 50 nM to 1 pM. Fluorescence was measured in 5 min intervals at 37 °C using an excitation of 410 nm and emission of 520 nm using the FLUOstar Omega plate reader (BMG Labtech).

Construction of *C. rodentium* mutant

C. rodentium strain ICC169 ΔnleF (ICC1129) was generated using a modified version of the lambda red-based mutagenesis system(42). Briefly, the *nleF* gene and its flanking regions were PCR-amplified from WT *C. rodentium* ICC169 genomic DNA using the primers pair NleF-up-Fw/NleF-down-Rv and cloned into pC-Blunt-TOPO vector (Invitrogen). The *nleF* gene was then excised using inverse-PCR (primers NleF-up-Rv-BamHI/NleF-down-Fw-BamHI) and the resulting linear product was BamHI digested, allowing insertion of the non-polar *aphT*(43), cassette, resulting in plasmid pICC1674. After verifying for correct orientation of the kanamycin cassette, the insert was PCR-amplified using NleF-up-Fw and NleF-down-Rv primers. The PCR products were electroporated into wild type *C. rodentium* expressing the lambda red recombinase from pKD46 plasmid. The deletion was confirmed by PCR and DNA sequencing amongst the kanamycin resistant clones (primers NleF-up-Fw-check and NleF-down-Fw-check).

Oral infection of mice

Pathogen-free female C57BL/6 mice were either purchased from Charles River or sourced from BIME Institut Pasteur. Casp*1/11*[-/-] mice were generously provided by Bernhard Ryffel (TAAM-CDTA, Orelans, France) and *Casp11*^{-/-} were generously provided by Mohamed Lamkanfi (Ghent University, Belgium). All animals were housed in individually HEPA-filtered cages with sterile bedding and free access to sterilized food and water. Independent infection experiments for wild-type C57BL/6, *Casp1/11*[-/-] and Casp*11*[-/-] mice were performed using 3 to 8 mice per group. Mice were infected and followed for shedding as described(44). Briefly, mice were infected via oral gavage with 10^9 WT *C. rodentium* or *C. rodentium ΔnleF* as described previously. For control, mice were gavaged with sterile PBS. The number of viable bacteria used as inoculum was determined by retrospective plating onto LB agar containing antibiotics. Stool samples were recovered aseptically at various time points after inoculation and the number of viable bacteria per gram of stool was determined by plating onto LB agar(44).

Sample collection and colonic crypt hyperplasia measurement

Segments of the terminal colon (0.5 cm) of each mouse were collected, flushed and fixed in 10% neutral buffered formalin. Formalin fixed tissues were then processed, paraffin-embedded, sectioned at 5 μm and stained with haematoxylin and eosin (H&E) using standard techniques. H&E stained tissues were evaluated for colonic crypt hyperplasia microscopically without knowledge of the treatment condition used in the study and the length of at least 100 well-oriented crypts from each section from all of the mice per treatment group (n=4-6) were evaluated. H&E stained tissues were imaged with an Axio Lab.A1 microscope (Carl Zeiss MicroImaging GmbH Germany), images were acquired using an Axio Cam ERc5s colour camera, and computer-processed using AxioVision (Carl Zeiss MicroImaging GmbH, Germany).

Sample collection for cytokine analysis and flow cytometry

Isolation of colonic cells and flow cytometry were performed as described(44). After a PBS wash, the 5th cm of the distal colon was incubated in RPMI containing penicillin, streptomycin, gentamicin and FBS at 37°C for 24 h. The concentrations of IL-18 (eBioscience, #BMS618/3), IL-1β and KC (CXCL1; R&D Systems) were determined by ELISA according to the manufacturer's protocols.

Statistics

All data was analyzed using GraphPad Prism software, using the Mann-Whitney test and represented as the mean +/- standard error of mean or standard deviation. A P value less than 0.05 (P<0.05) was considered statistically significant.

Supplementary Materials

Refer to Web version on PubMed Central for supplementary material.

Acknowledgements

References

(1). Croxen MA, Law RJ, Scholz R, Keeney KM, Wlodarska M, Finlay BB. Recent advances in understanding enteric pathogenic *Escherichia coli*. Clin Microbiol Rev. 2013; 26:822–880. [PubMed: 24092857]

(2). Collins JW, Keeney KM, Crepin VF, Rathinam VA, Fitzgerald KA, Finlay BB, et al. *Citrobacter rodentium*: infection, inflammation and the microbiota. Nat Rev Microbiol. 2014; 12:612–623. [PubMed: 25088150]

(3). Baruch K, Gur-Arie L, Nadler C, Koby S, Yerushalmi G, Ben-Neriah Y, et al. Metalloprotease type III effectors that specifically cleave JNK and NF-kappaB. EMBO J. 2011; 30:221–231. [PubMed: 21113130]

(4). Zhang L, Ding X, Cui J, Xu H, Chen J, Gong Y, et al. Cysteine methylation disrupts ubiquitin-chain sensing in NF-κB activation. Nature. 2011; 481:204–208. [PubMed: 22158122]

(5). Pearson JS, Riedmaier P, Marchès O, Frankel G, Hartland EL. A type III effector protease NleC from enteropathogenic *Escherichia coli* targets NF-?B for degradation. Mol Microbiol. 2011; 80:219–230. [PubMed: 21306441]

(6). Li S, Zhang L, Yao Q, Li L, Dong N, Rong J, et al. Pathogen blocks host death receptor signalling by arginine GlcNAcylation of death domains. Nature. 2013; 501:242–246. [PubMed: 23955153]

(7). Pham TH, Gao X, Singh G, Hardwidge PR. Escherichia coli virulence protein NleH1 interaction with the v-Crk sarcoma virus CT10 oncogene-like protein (CRKL) governs NleH1 inhibition of the ribosomal protein S3 (RPS3)/nuclear factor kappaB (NF-kappaB) pathway. J Biol Chem. 2013; 288:34567–34574. [PubMed: 24145029]

(8). von Moltke J, Ayres JS, Kofoed EM, Chavarria-Smith J, Vance RE. Recognition of bacteria by inflammasomes. Annu Rev Immunol. 2013; 31:73–106. [PubMed: 23215645]

(9). Eldridge MJ, Shenoy AR. Antimicrobial inflammasomes: unified signalling against diverse bacterial pathogens. Curr Opin Microbiol. 2015; 23:32–41. [PubMed: 25461570]

(10). Shi J, Zhao Y, Wang Y, Gao W, Ding J, Li P, et al. Inflammatory caspases are innate immune receptors for intracellular LPS. Nature. 2014; 514:187–192. [PubMed: 25119034]

(11). Kayagaki N, Warming S, Lamkanfi M, Vande Walle L, Louie S, Dong J, et al. Non-canonical inflammasome activation targets caspase-11. Nature. 2011; 479:117–121. [PubMed: 22002608]

(12). Casson CN, Yu J, Reyes VM, Taschuk FO, Yadav A, Copenhaver AM, et al. Human caspase-4 mediates noncanonical inflammasome activation against gram-negative bacterial pathogens. Proc Natl Acad Sci U S A. 2015; 112:6688–6693. [PubMed: 25964352]

(13). Rathinam VA, Vanaja SK, Waggoner L, Sokolovska A, Becker C, Stuart LM, et al. TRIF licenses caspase-11-dependent NLRP3 inflammasome activation by gram-negative bacteria. Cell. 2012; 150:606–619. [PubMed: 22819539]

(14). Knodler LA, Crowley SM, Sham HP, Yang H, Wrande M, Ma C, et al. Noncanonical inflammasome activation of caspase-4/caspase-11 mediates epithelial defenses against enteric bacterial pathogens. Cell Host Microbe. 2014; 16:249–256. [PubMed: 25121752]

(15). Hemrajani C, Berger CN, Robinson KS, Marches O, Mousnier A, Frankel G. NleH effectors interact with Bax inhibitor-1 to block apoptosis during enteropathogenic *Escherichia coli* infection. Proc Natl Acad Sci U S A. 2010; 107:3129–3134. [PubMed: 20133763]

(16). Liu Z, Zaki MH, Vogel P, Gurung P, Finlay BB, Deng W, et al. Role of inflammasomes in host defense against *Citrobacter rodentium* infection. J Biol Chem. 2012; 287:16955–16964. [PubMed: 22461621]

(17). Song-Zhao GX, Srinivasan N, Pott J, Baban D, Frankel G, Maloy KJ. Nlrp3 activation in the intestinal epithelium protects against a mucosal pathogen. Mucosal Immunol. 2014; 7:763–774. [PubMed: 24280937]

(18). Yen H, Sugimoto N, Tobe T. Enteropathogenic *Escherichia coli* Uses NleA to Inhibit NLRP3 Inflammasome Activation. PLoS Pathog. 2015; 11:e1005121. [PubMed: 26332984]

(19). Blasche S, Mortl M, Steuber H, Siszler G, Nisa S, Schwarz F, et al. The *E. coli* Effector Protein NleF Is a Caspase Inhibitor. PLoS ONE. 2013; 8:e58937. [PubMed: 23516580]

(20). Pallett MA, Berger CN, Pearson JS, Hartland EL, Frankel G. The type III secretion effector NleF of enteropathogenic *Escherichia coli* activates NF-kappaB early during infection. Infect Immun. 2014; 82:4878–4888. [PubMed: 25183730]

(21). Dinarello CA, Fantuzzi G. Interleukin-18 and host defense against infection. J Infect Dis. 2003; 187(Suppl 2):S370–84. [PubMed: 12792854]

(22). Brodsky IE, Palm NW, Sadanand S, Ryndak MB, Sutterwala FS, Flavell RA, et al. A Yersinia effector protein promotes virulence by preventing inflammasome recognition of the type III secretion system. Cell Host Microbe. 2010; 7:376–387. [PubMed: 20478539]

(23). Hagar JA, Powell DA, Aachoui Y, Ernst RK, Miao EA. Cytoplasmic LPS activates caspase-11: implications in TLR4-independent endotoxic shock. Science. 2013; 341:1250–1253. [PubMed: 24031018]

(24). Kobayashi T, Ogawa M, Sanada T, Mimuro H, Kim M, Ashida H, et al. The Shigella OspC3 effector inhibits caspase-4, antagonizes inflammatory cell death, and promotes epithelial infection. Cell Host Microbe. 2013; 13:570–583. [PubMed: 23684308]

(25). Gurung P, Malireddi RK, Anand PK, Demon D, Vande Walle L, Liu Z, et al. Toll or interleukin-1 receptor (TIR) domain-containing adaptor inducing interferon-beta (TRIF)-mediated caspase-11 protease production integrates Toll-like receptor 4 (TLR4) protein- and Nlrp3 inflammasome-mediated host defense against enteropathogens. J Biol Chem. 2012; 287:34474–34483. [PubMed: 22898816]

(26). Verri WA Jr, Cunha TM, Ferreira SH, Wei X, Leung BP, Fraser A, et al. IL-15 mediates antigen-induced neutrophil migration by triggering IL-18 production. Eur J Immunol. 2007; 37:3373–3380. [PubMed: 17979156]

(27). Canetti CA, Leung BP, Culshaw S, McInnes IB, Cunha FQ, Liew FY. IL-18 enhances collagen-induced arthritis by recruiting neutrophils via TNF-alpha and leukotriene B4. J Immunol. 2003; 171:1009–1015. [PubMed: 12847274]

(28). Dupaul-Chicoine J, Yeretssian G, Doiron K, Bergstrom KS, McIntire CR, LeBlanc PM, et al. Control of intestinal homeostasis, colitis, and colitis-associated colorectal cancer by the inflammatory caspases. Immunity. 2010; 32:367–378. [PubMed: 20226691]

(29). Daig R, Rogler G, Aschenbrenner E, Vogl D, Falk W, Gross V, et al. Human intestinal epithelial cells secrete interleukin-1 receptor antagonist and interleukin-8 but not interleukin-1 or interleukin-6. Gut. 2000; 46:350–358. [PubMed: 10673296]

(30). Basu R, O'Quinn DB, Silberger DJ, Schoeb TR, Fouser L, Ouyang W, et al. Th22 cells are an important source of IL-22 for host protection against enteropathogenic bacteria. Immunity. 2012; 37:1061–1075. [PubMed: 23200827]

(31). Knodler LA, Crowley SM, Sham HP, Yang H, Wrande M, Ma C, et al. Noncanonical inflammasome activation of caspase-4/caspase-11 mediates epithelial defenses against enteric bacterial pathogens. Cell Host Microbe. 2014; 16:249–256. [PubMed: 25121752]

(32). Verri WA Jr, Cunha TM, Ferreira SH, Wei X, Leung BP, Fraser A, et al. IL-15 mediates antigen-induced neutrophil migration by triggering IL-18 production. Eur J Immunol. 2007; 37:3373–3380. [PubMed: 17979156]

(33). Canetti CA, Leung BP, Culshaw S, McInnes IB, Cunha FQ, Liew FY. IL-18 enhances collagen-induced arthritis by recruiting neutrophils via TNF-alpha and leukotriene B4. J Immunol. 2003; 171:1009–1015. [PubMed: 12847274]

(34). Spehlmann ME, Dann SM, Hruz P, Hanson E, McCole DF, Eckmann L. CXCR2-dependent mucosal neutrophil influx protects against colitis-associated diarrhea caused by an attaching/effacing lesion-forming bacterial pathogen. J Immunol. 2009; 183:3332–3343. [PubMed: 19675161]

(35). Elinav E, Henao-Mejia J, Flavell RA. Integrative inflammasome activity in the regulation of intestinal mucosal immune responses. Mucosal Immunol. 2013; 6:4–13. [PubMed: 23212196]

(36). Wlodarska M, Thaiss CA, Nowarski R, Henao-Mejia J, Zhang JP, Brown EM, et al. NLRP6 inflammasome orchestrates the colonic host-microbial interface by regulating goblet cell mucus secretion. Cell. 2014; 156:1045–1059. [PubMed: 24581500]

(37). Allen IC. Non-Inflammasome Forming NLRs in Inflammation and Tumorigenesis. Front Immunol. 2014; 5:169. [PubMed: 24795716]

(38). Nordlander S, Pott J, Maloy KJ. NLRC4 expression in intestinal epithelial cells mediates protection against an enteric pathogen. Mucosal Immunol. 2014; 7:775–785. [PubMed: 24280936]

(39). Fellmann C, Hoffmann T, Sridhar V, Hopfgartner B, Muhar M, Roth M, et al. An optimized microRNA backbone for effective single-copy RNAi. Cell Rep. 2013; 5:1704–1713. [PubMed: 24332856]

(40). Shenoy AR, Wellington DA, Kumar P, Kassa H, Booth CJ, Cresswell P, et al. GBP5 promotes NLRP3 inflammasome assembly and immunity in mammals. Science. 2012; 336:481–485. [PubMed: 22461501]

(41). Kotik-Kogan O, Valentine ER, Sanfelice D, Conte MR, Curry S. Structural analysis reveals conformational plasticity in the recognition of RNA 3' ends by the human La protein. Structure. 2008; 16:852–862. [PubMed: 18547518]

(42). Datsenko KA, Wanner BL. One-step inactivation of chromosomal genes in Escherichia coli K-12 using PCR products. Proc Natl Acad Sci U S A. 2000; 97:6640–6645. [PubMed: 10829079]

(43). Galan JE, Ginocchio C, Costeas P. Molecular and functional characterization of the Salmonella invasion gene invA: homology of InvA to members of a new protein family. J Bacteriol. 1992; 174:4338–4349. [PubMed: 1624429]

(44). Crepin VF, Habibzay M, Glegola-Madejska I, Guenot M, Collins JW, Frankel G. Tir Triggers Expression of CXCL1 in Enterocytes and Neutrophil Recruitment during Citrobacter rodentium Infection. Infect Immun. 2015; 83:3342–3354. [PubMed: 26077760]
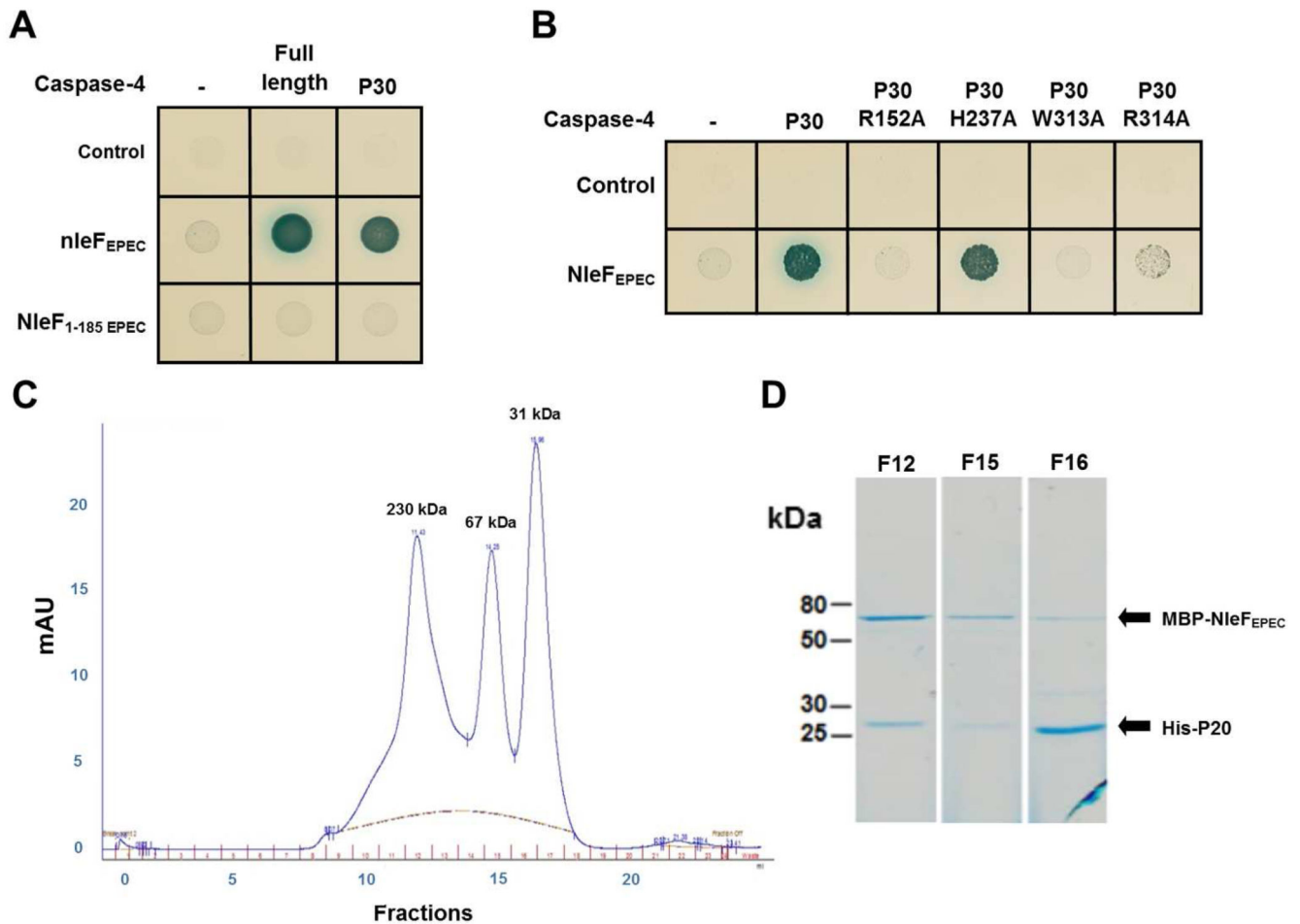
Fig. 1. NleF binds caspase-4.
(A) A direct yeast two hybrid assay revealed that $NleF_{EPEC}$, but not $NleF_{1-185\_EPEC}$, interacts with full-length and p30 caspase-4. (B) Substitution of amino acids R152A, W313A and R314A within the putative caspase-4 substrate domain abrogated the interaction with $NleF_{EPEC}$. (C) Fractions of size exclusion of the chromatographic profile of MBP-$NleF_{EPEC}$ and His-p20/p10 caspase-4 purified by amylose and talon affinity chromatography and (D) analyzed by SDS-PAGE gel electrophoresis, revealed that $NleF_{EPEC}$ and caspase-4 subunits co-purified and co-eluted as a macromolecular complex at a MW of ~230 kDa.
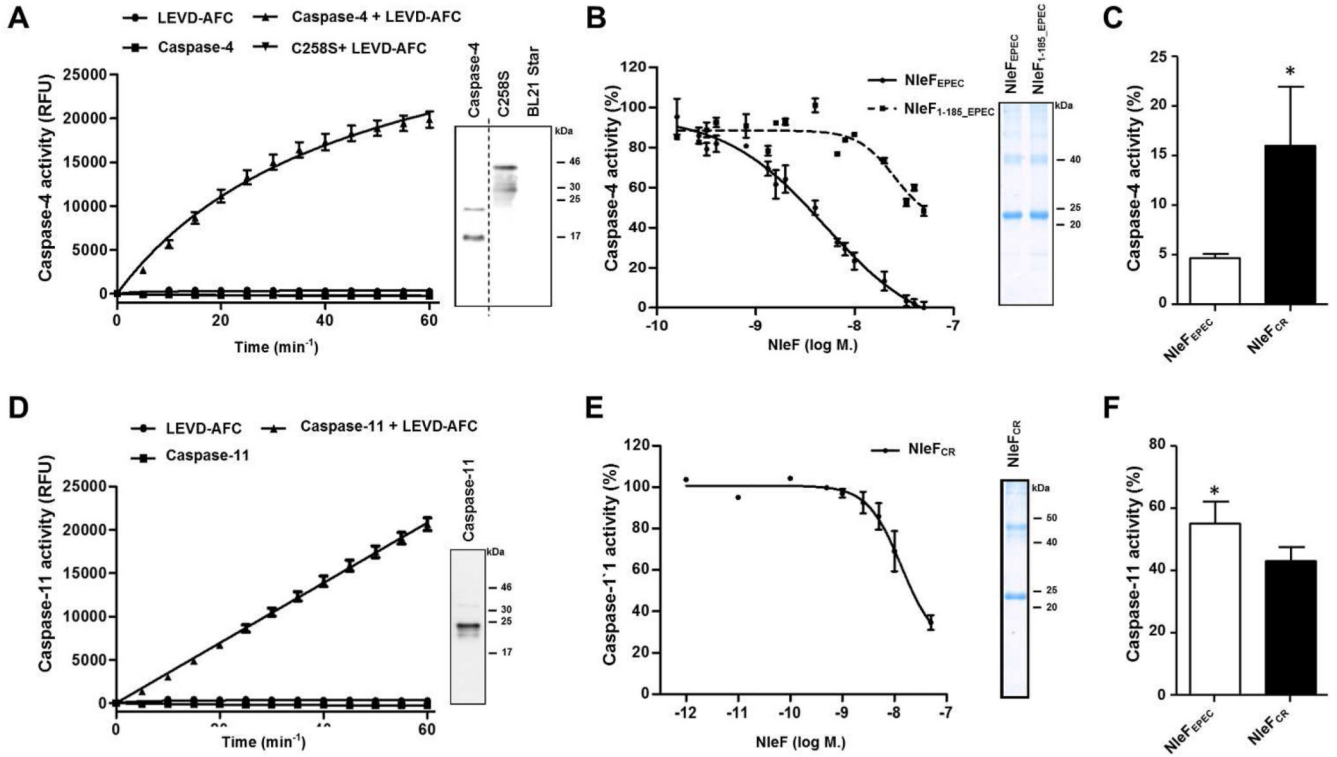
Fig. 2. NleF inhibits caspase-4 activity.
(A) Recombinant caspase-4, but not caspase-4^{C258S}, is auto-activated (western blot) and cleaves the reporter Ac-LEVD-AFC. Results are plotted as relative fluorescence units (RLU) minus background (No Ac-LEVD-AFC) over time (min). (B) Dose-dependent inhibition of caspase-4 Ac-LEVD-AFC cleavage by recombinant NleF$_{EPEC}$, and NleF$_{1-185\_EPEC}$ (shown by Coomassie stained gel). (C) NleF$_{EPEC}$ (10 nM) inhibits the activity of caspase-4 more efficiently than NleF$_{CR}$ (10nM) after 30 min incubation in the presence of Ac-LEVD-AFC. (D) Recombinant caspase-11 is auto-activated (western blot) and cleaves the reporter Ac-LEVD-AFC. (E) Dose dependent inhibition of caspase-11 activity by recombinant NleF$_{CR}$ (shown by Coomassie stained gel). (F) NleF$_{CR}$ (50 nM) inhibits the activity of caspase-11 more efficiently than NleF$_{EPEC}$ (50nM) after 30 min incubation in the presence of Ac-LEVD-AFC. Results are expressed as a percentage of wild-type caspase-4 or caspase-11 RLU/min from at least two independent experiments. * indicates P<0.05.
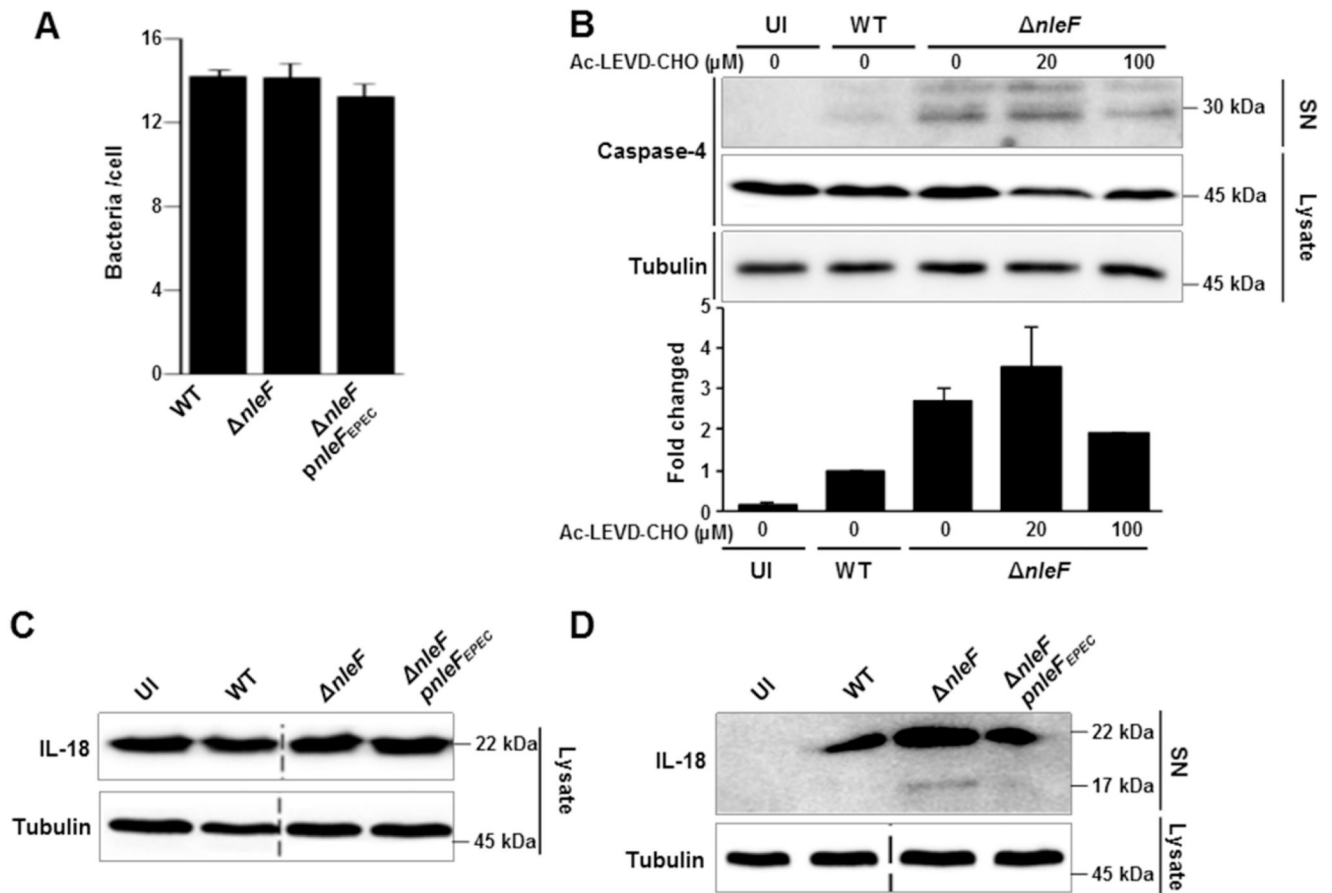
Fig. 3. NleF inhibits secretion of caspase-4 and IL-18 during EPEC infection.
(A) Infection of polarized Caco-2 cells with WT EPEC, EPEC Δ*nleF* or the complemented strain (*pnleF*$_{EPEC}$) revealed similar levels of cell adhesion (3 h post infection). **(B)** Caco-2 cells were infected with WT EPEC or EPEC Δ*nleF* in the absence or presence of the inhibitor Ac-LEVD-CHO (total 21 h). Immunoblotting of supernatants (SN) revealed that EPEC inhibits secretion of active caspase-4 (~28 kDa) in an NleF$_{EPEC}$-dependent manner, assessed by western blots (upper panel) and quantified by densitometry of multiple experiments (lower panel). **(C)** Infection of Caco-2 cells with WT EPEC, EPEC Δ*nleF* or complemented EPEC Δ*nleF* (*pnleF*$_{EPEC}$) had no effect on the levels of total IL-18 at 4 h p.i. **(D)** NleF is essential for inhibition of IL-18 secretion from infected Caco-2 cells (21 h post infection).
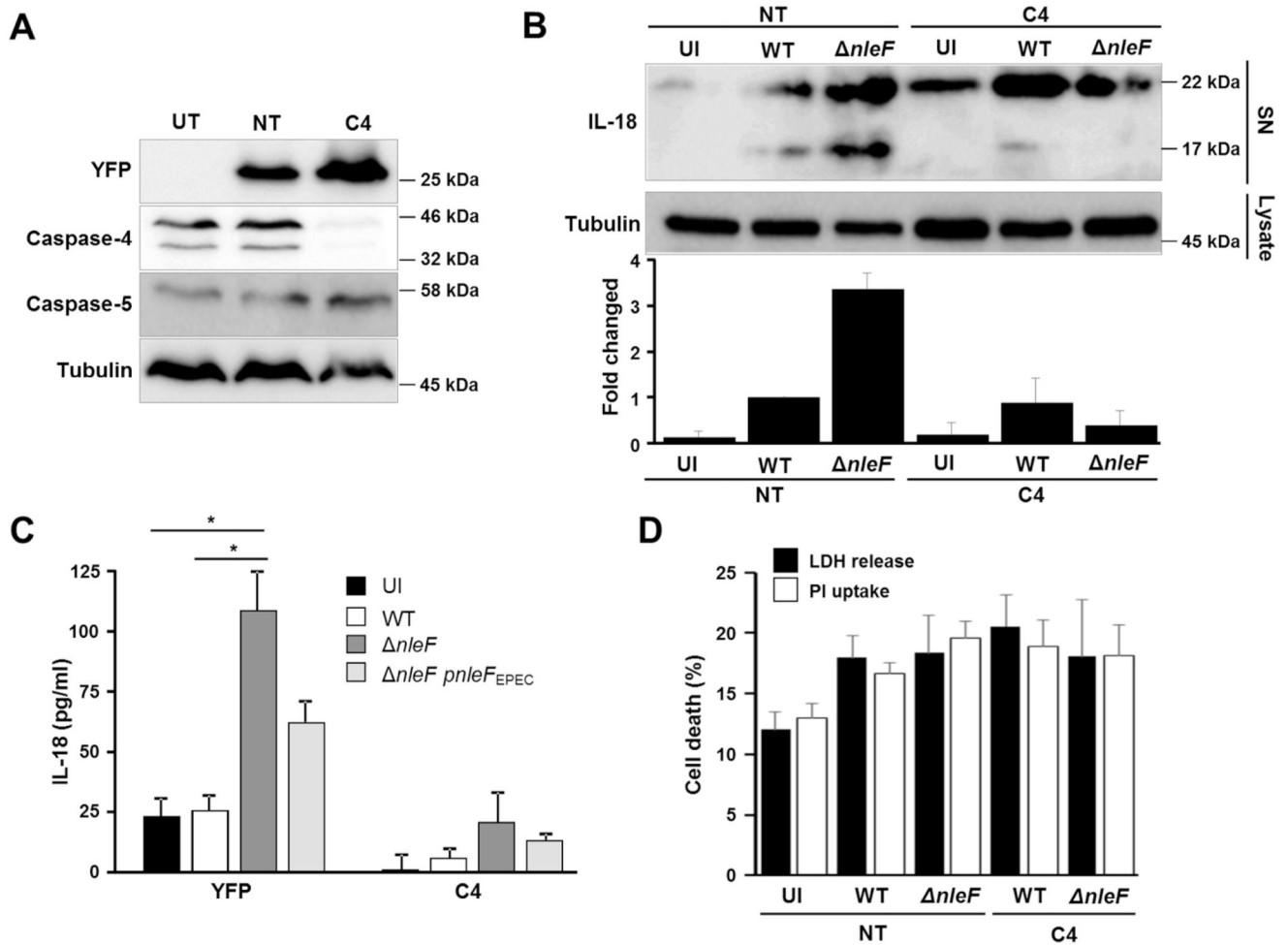
Fig. 4. NleF$_{EPEC}$ inhibits IL-18 secretion in an caspase-4 dependent manner.
(**A**) Western blots showing knockdown of caspase-4, but not capsapse-5, by miRNA30E. (**B**) Infection of Caco-2 cells (21 h) depleted of caspase-4 (C4) revealed that it is essential for IL-18 processing in response to infection with EPEC *nleF*, assessed by western blots (upper panel) and quantified by densitometry of two independent experiments (lower panel). (**C**) ELISA from two biological repeats showing specific secretion of IL-18 from control (YFP), but not from C4, Caco-2 cells infected for 21 h with EPEC *nleF*. (**D**) EPEC does not trigger LDH release or PI uptake during infection (21 h) of control or C4 Caco-2 cells, results are represented as a percentage of total uptake or total release and are an average of two biological repeats carried out in triplicate. * indicates P<0.05.
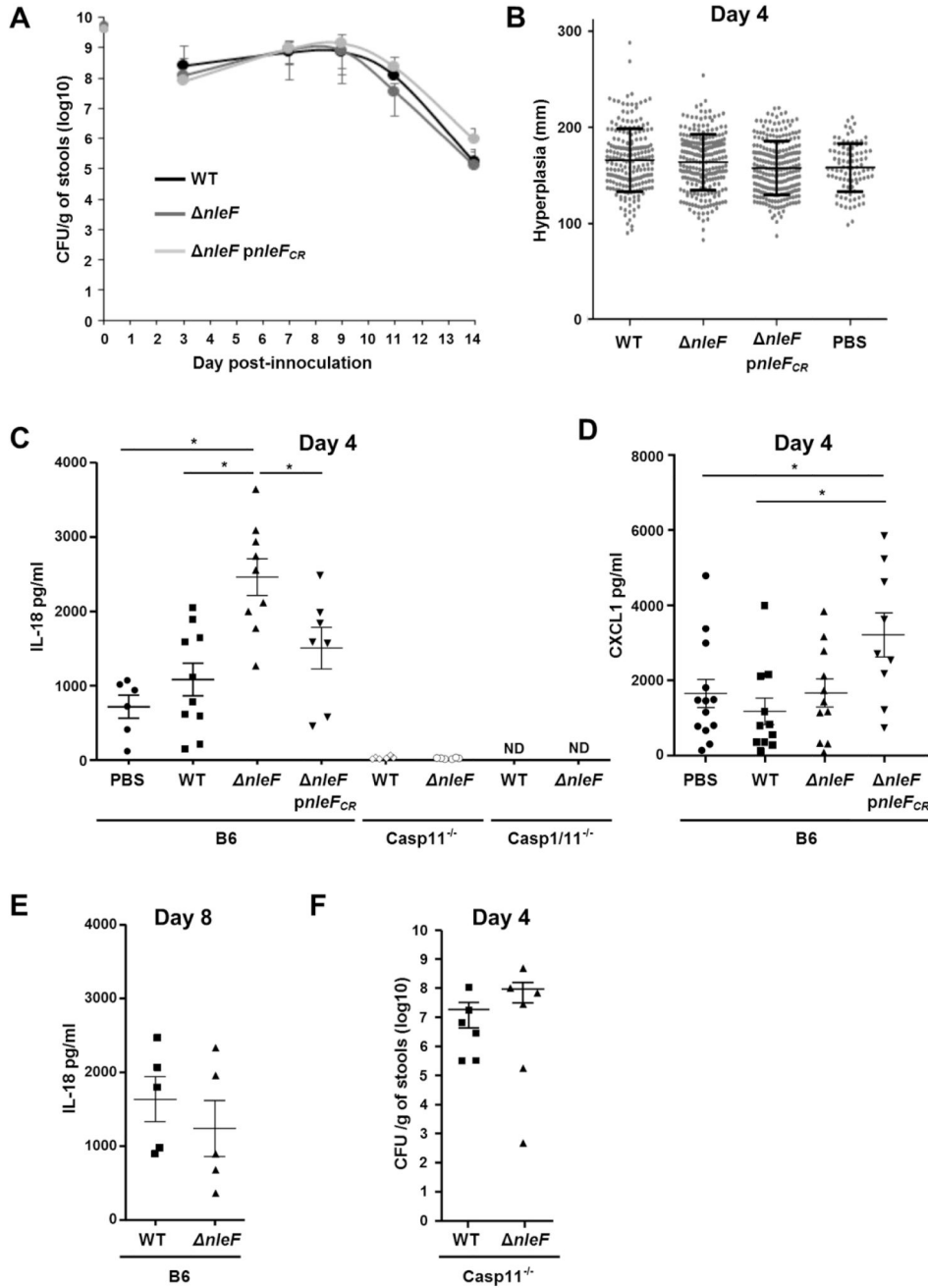
Fig. 5. NleF$_{CR}$ inhibits colonic IL18 secretion 4 days p.i.
WT *C. rodentium*, *C. rodentium* *nleF* and the complemented strain (*nleF* p*nleF*CR)
similarly colonized and triggered colonic hypoplasia in C57BL/6 mice (**A and B**). Each dot
in B represents an individual measurement of crypt length (from at least 20 measurements
per section per mouse), and horizontal bars represent mean values. Significant increase in
secreted IL-18, measured by ELISA, was seen specifically following infection of C57BL/6
with *C. rodentium* *nleF* (day 4), but not following infection of either *Casp1/11$^{-/-}$* or
Casp11$^{-/-}$ mice (day 4) (**C**) or C57BL/6 (day 8) (**E**). Secreted CXCL1 was found in similar

levels, except for the complemented strain, which triggered greater secretion of CXCL1 **(D)**. No difference in colonization of *Casp11*$^{-/-}$ mice was seen following infection with WT *C. rodentium* or *C. rodentium* Δ*nleF* (E). ***** indicates P<0.05.
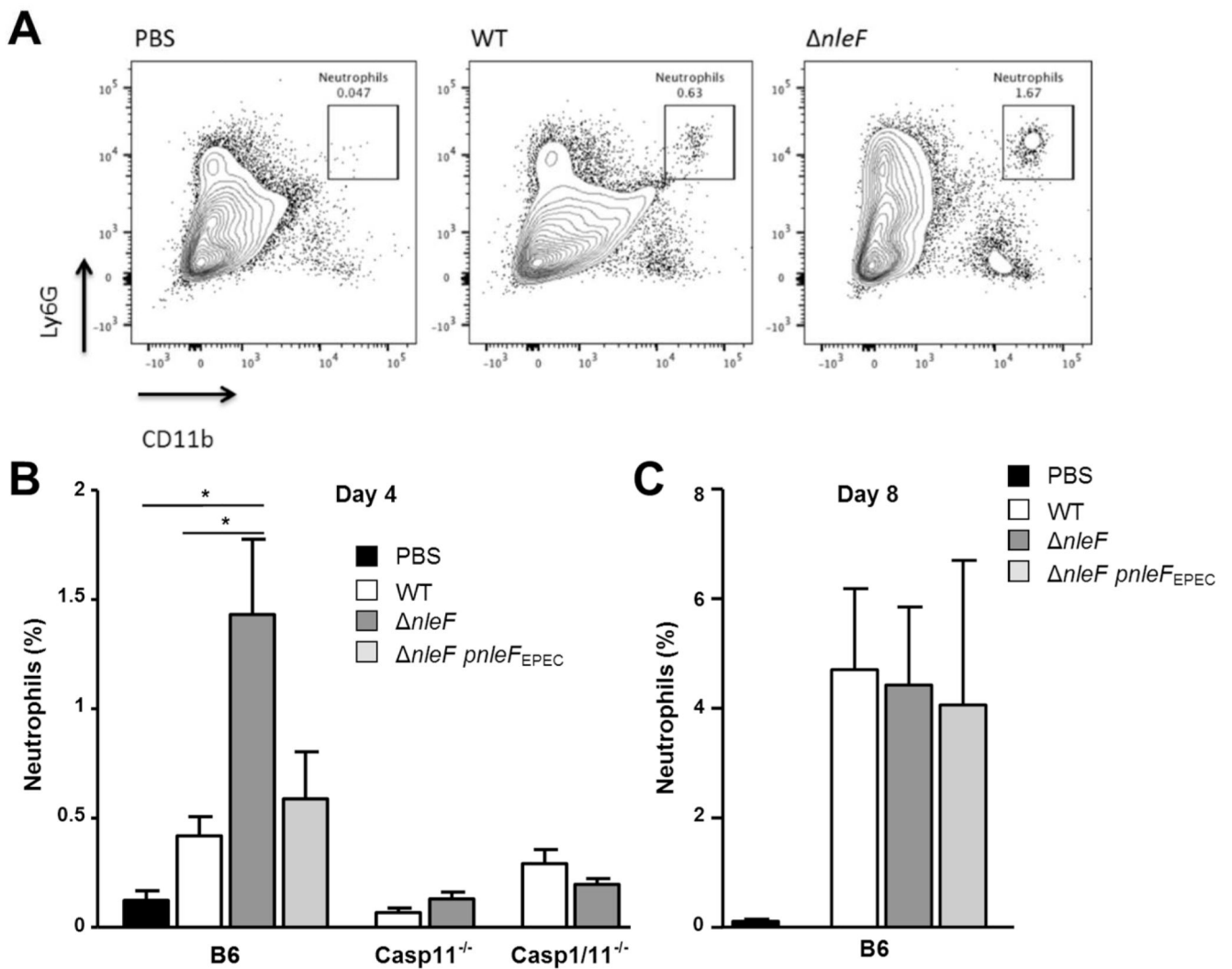
Fig. 6. NleF$_{CR}$ inhibits colonic neutrophil recruitment 4 days p.i.
C57BL/6, *Casp1/11$^{-/-}$* and *Casp11$^{-/-}$* mice were infected with WT *C. rodentium*, *C. rodentium* ΔnleF or complemented *C. rodentium* ΔnleF (ΔnleF pnleFCR). **(A)** Representative image of flow cytometry gating strategy for neutrophils (CD11b+Ly6G+) of control (PBS) and infected C57BL/6 mice. The number of neutrophils (CD11b+Ly6G+) present within the myeloid gate was counted from C57BL/6 (**B-C**, days 4 and 8 post infection), *Casp1/11$^{-/-}$* or *Casp11$^{-/-}$* (**B**, day 4 post infection) mice (at least six mice per condition). ***** indicates P<0.05.